# Basic research of HTS coil cooling assist technology by magnetic refrigeration



# Basic research of HTS coil cooling assist technology by magnetic refrigeration

Journal of Physics: Conference Series **1559** (2020) 012090 doi:10.1088/1742-6596/1559/1/012090

# Basic research of HTS coil cooling assist technology by magnetic refrigeration

**Naoki HIRANO[(a)], Setsura NAGAI [(b)], Yunzhi XIE [(b)], Tetsuji. OKAMURA [(b)]**

[(a)] National Institute for Fusion Science
322-6 Orishi-cho, Toki-shi, Gifu, Japan
[(b)] Department of Energy Sciences, Tokyo Institute of Technology
Nakatsuda-cho, Midori-ku, Yokohama, Japan

hirano.naoki@nifs.ac.jp

**Abstract.** The fundamental research of HTS coil cooling assist technology by magnetic refrigeration has been studied. Using magnetic refrigeration technology, we are focusing on numerical analysis to see if the cooling efficiency around 20 K of high-temperature superconducting coils can be enhanced. The feature of the proposed cooling method is that it utilizes the leakage magnetic field from the HTS coil. Magnetic refrigeration technology needs to apply a change of magnetic field to a certain type of magnetic material, and the configuration of applying a change of magnetic field to the material in the cryostat is the point of the proposed cooling assist method. We confirm a system that uses a magnetic refrigerator in combination with a refrigerant circulation cooling system by utilizing the leakage magnetic field generated when using a superconducting coil and producing a magneto caloric effect has higher refrigeration performance than the refrigerant circulation cooling system alone.

## 1. Introduction

Recently, it has become difficult to supply helium, which has affected cryogenic experiments. For this reason, we started the development of a cryogenic system that does not rely on helium. As a method for obtaining a low temperature around 20K, it is considered to circulate gas. As a method for obtaining a low temperature around 20K, it is considered to circulate hydrogen gas. In addition, we are studying combinations with magnetic refrigeration technology that can be expected to operate with high efficiency. In this presentation, we report on the analysis of the improvement in cooling performance by combining magnetic refrigeration and circulating cooling. In addition, we are studying combinations with magnetic refrigeration technology that can be expected to operate with high efficiency. In this presentation, we report on the analysis of the improvement in cooling performance by combining magnetic refrigeration and circulating cooling.

## 2. Gas circulation cooling

A schematic diagram of the gas circulation cooling system is shown in figure1. The main components are a compressor, a counter-flow type precooling heat exchanger, a GM refrigerator, and a part to be cooled. In this system, normal temperature gas enters the cryostat from the compressor, and heat is exchanged in the cold head section of the counter-flow type cold heat exchanger and GM refrigerator, and cooled to the 20 K level. Then, after receiving heat from the heat input section, it circulates again through the flow path that returns to the compressor through the counter flow type precooling heat

exchanger. Since the GM refrigerator and the part to be cooled are assumed to be used separately, the part to be cooled is outside the cryostat containing the GM refrigerator and is connected by a heat insulating tube wrapped with a radiation shield.

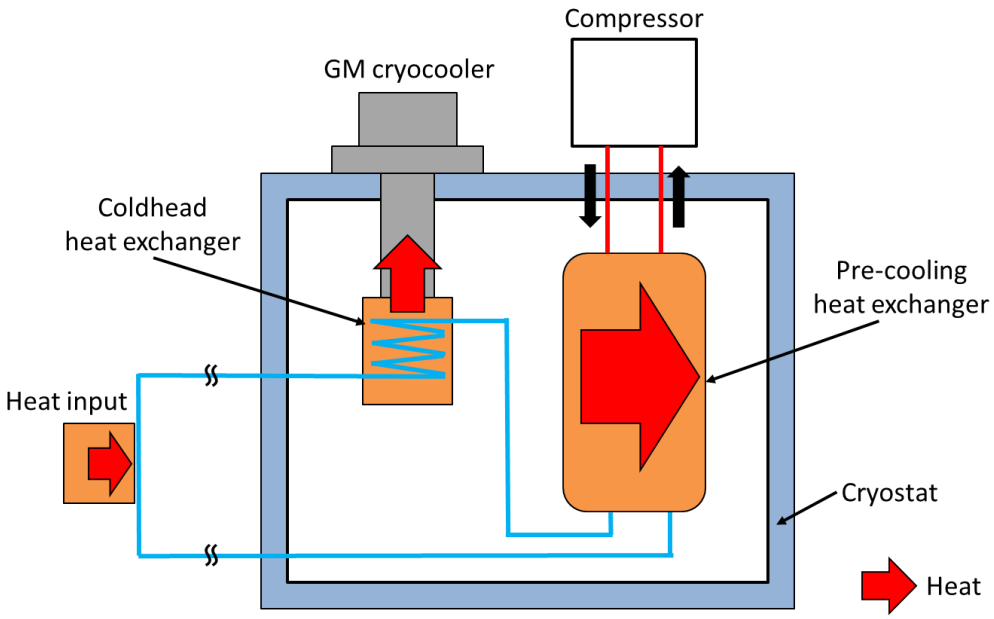


**Figure 1.** Schematic of gas circulation cooling system.

## 3. Numerical analysis of the gas circulation cooling system

### *3.1. One-dimensional numerical analysis model and corresponding components*

The numerical analysis of the gas circulation cooling system is a one-dimensional model of the counter-flow spiral double-pipe heat exchanger, GM refrigerator cold head heat exchanger, and heat input section, which are components of the cooling system, and solves the governing equations. The numbers in the left and right figures in figure 2 are the corresponding system components.

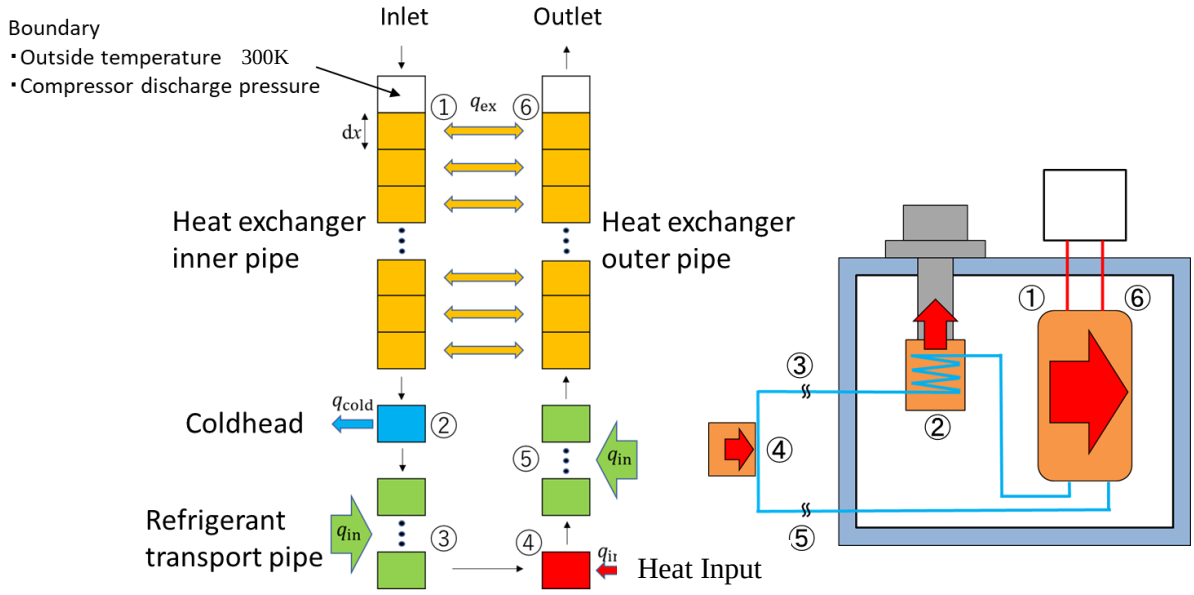


**Figure 2.** One-dimensional numerical analysis model and corresponding components

*3.2. Basic equations*

In the analysis model, the flow path was divided into small sections $d_x$ in the direction of refrigerant flow, and the analysis was performed using the energy conservation equation (1) as the governing equation for each inspection analysis. ρ is density [kg / m$^3$], $c_p$ is constant pressure specific heat [J / (kg · K)], T is refrigerant temperature [K], t is time [s], u is refrigerant flow velocity [m / s], $q_{ex}$ is the amount of exchange heat per unit time [W] for each component ($q_{ex}$, $q_{cold}$, $q_{in}$, $q_{input}$ in Figure 2), S is the cross-sectional area [m$^2$], and k is the thermal conductivity [W / (m · K)]. The first term on the left side of equation (1) represents the time change of the temperature in the examination volume, and the second term on the left side represents the temperature change due to the movement of fluid from outside the examination volume. In equation (1), the first term on the right side represents heat exchange occurring in each test volume, the second term on the right side represents heat conduction from the adjacent test volumes, and the third term on the right side represents heat generation due to fluid friction.

$$\rho c_p \left(\frac{\partial T}{\partial t} + u\frac{\partial T}{\partial x}\right) = -\frac{q_{ex}}{S\mathrm{d}x} + k\frac{\partial^2 T}{\partial x^2} + u\frac{\partial P}{\partial x} \quad (1)$$

This governing equation was solved numerically by the difference method. Equation (2) shows the difference equation of Equation (1). However, $T_{(i,\,n)}$ is the temperature [K] in the i-th time step and n-th section (inspection volume). Δ P is the pressure loss [Pa] due to friction per time step, calculated using Darcy-Weisbach equation (3). F is the friction loss coefficient [-], D is the hydraulic diameter [m] Q is analyzed using equation (4) considering that the fluid continues to flow during one-time step. Q_n is the nth interval (inspection volume). The amount of heat exchanged, dt, represents the time step [s] at the time of analysis.

$$\rho c_p \left(\frac{T_{i+1,n}-T_{i,n}}{\mathrm{d}t} + u\frac{T_{i,n}-T_{i,n-1}}{\mathrm{d}x}\right) = -\frac{q_{ex}}{S\mathrm{d}x} + k\frac{T_{i,n+1}-2T_{i,n}+T_{i,n-1}}{(dx)^2} + u\frac{\Delta P}{\mathrm{d}x} \quad (2)$$

$$\Delta P = f * \frac{u\mathrm{d}t}{D} * \frac{\rho u^2}{2} \quad (3)$$

$$q_{ex} = q_n(\mathrm{d}x - 0.5u\mathrm{d}t) + q_{n-1} * 0.5u\mathrm{d}t \quad (4)$$

*3.3. Conditions for numerical analysis*

The conditions of the numerical analysis are shown in Table 1. Here, $\Delta T_{ref}$, $\Delta T_{coil}$, and $\Delta T_{mid}$ are temperature changes in the cold head heat exchanger, heat input section, and heat exchanger intermediate section in one-time step. In this analysis, the gas was helium.

**Table 1** The conditions of the numerical analysis

| | |
|---|---|
| Time mesh size *dt* | 0.001 s |
| Spatial mesh size *dx* | 0.1 m |
| Compressor discharge pressure | 1.0 ~ 2.0 MPa |
| Heat exchanger inlet boundary temperature | 300 K |
| Refrigerator cold head initial temperature | 100 ~ 300 K |
| Mass flow rate | 0.1 ~ 2.0 g/s |
| Heat exchanger one way length | 60 m |
| Steady condition | $\Delta T_{ref}, \Delta T_{coil}, \Delta T_{mid} < 10^{-7}\ K$<br>More than $10^5$calculations |
| GM refrigerator | RDK-520E<br>Made by Sumitomo Heavy Industries |

The flow chart of the numerical analysis is shown in Figure 3. As initial conditions, the helium filling pressure, the helium temperature of each mesh, the mass flow rate, and the heat input at the heat input section are set, and then the physical properties are calculated from the pressure and temperature. After that, the heat exchange amount and friction loss coefficient in each mesh are calculated, and then the energy conservation equation is solved. Further, whether or not it is steady is judged, and if it is not steady, it is calculated again from the physical property values. The numerical analysis ends when the steady condition is satisfied.

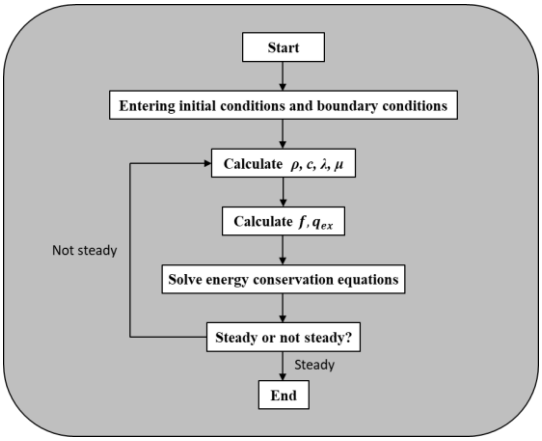


**Figure 3.** The flow chart of the numerical analysis.

*3.4. Numerical analysis results*

The analysis result of the temperature of the object to be cooled with respect to the heat load when the mass flow rate is fixed at 1.0 g/s and the compressor discharge pressure is set as a parameter (1.0, 1.2, 1.4, 1.6, 1.8, 2.0 MPa) is shown in Figure 4. Figure 5 shows the analysis results of the cooled object temperature with respect to the thermal load when the compressor discharge pressure is fixed at 1.5 MPa and the mass flow rate is set as a parameter (0.5, 1.0, 1.5, 2.0 g/s). Figure 6 shows the temperature distribution and pressure distribution of the entire flow path when the mass flow rate is a parameter and the heat load is 0 W. In figure 6, 0 to 60 m is the inner tube of the double tube precooling heat exchanger, 60.1 m is the GM refrigerator cold head heat exchanger, 60.2 m is the object to be cooled, 60.3 to 120.3 m is the outer tube of the double-tube precooling heat exchanger. The solid and dotted lines in Fig. 6 correspond to the flow rate.

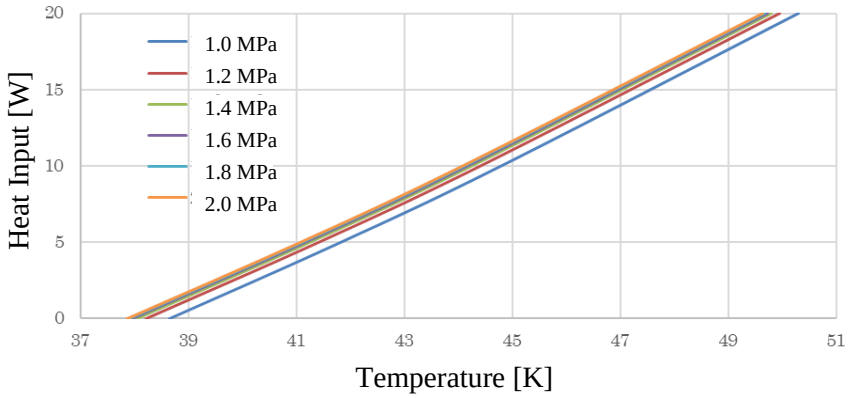


**Figure 4.** Analysis results of the temperature of the cooled part with respect to the heat load when the mass flow rate is fixed at 1.0 g/s and the compressor discharge pressure is set as a parameter.

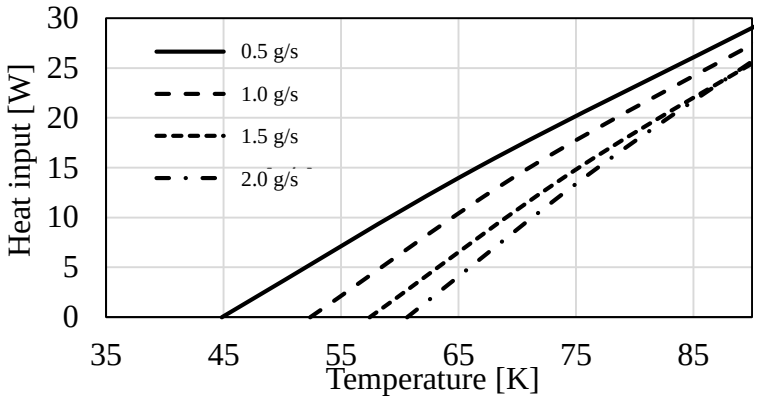


**Figure 5.** Analysis result of the temperature of the cooled part with respect to the heat load when the compressor discharge pressure is fixed at 1.5 MPa and the mass flow rate is set as a parameter

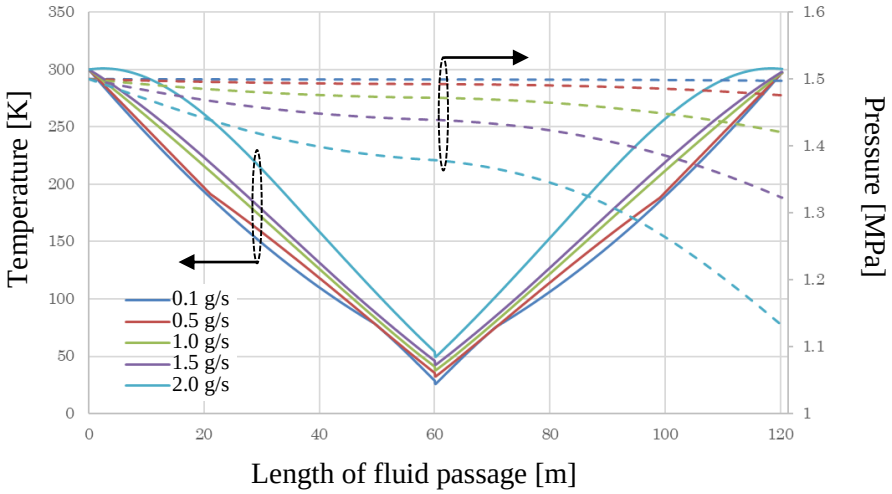


**Figure 6.** The temperature distribution and pressure distribution of the entire flow path when the mass flow rate is a parameter and the heat load is 0 W

It can be seen that there is an optimum flow rate according to the heat load, and it becomes larger as the heat load increases. Looking at the pressure distribution in the figure, it can be seen that the pressure loss increases as the flow rate increases. The increase in the pressure loss means that the amount of heat generated by the friction of the fluid also increases. From the temperature distribution at 2.0 g/s, the gas temperature in the heat exchanger rises significantly. The reason why the heat exchanger part of the graph of 0.1 g/s and 0.5 g/s is unnatural is that the flow rate is small. If the flow rate is small, heat is transmitted slowly, and the steady condition is satisfied in a state where the entire channel is not steady.

## 4. Numerical analysis results of cryogenic refrigerant circulation system using magnetic refrigeration

### *4.1. Magnetic refrigeration*

Magnetic refrigeration technology is an environment-friendly technology that does not use refrigerant which causes global warming. In addition, since operation close to an ideal refrigeration cycle is possible, there is a possibility that an efficient cooling device can be realized. Therefore, in recent years, expectations for magnetic refrigeration technology are increasing. There are already many reports about the prototyping of a heat pump around room temperature using magnetic refrigeration technology [1]-[4]. We have started research to apply this magnetic refrigeration technology to high-temperature superconducting coil cooling. The cooling temperature zone is 20-40 K. Since cooling from room temperature to this temperature zone with magnetic refrigeration technology alone is not practical, we

examined a system that takes charge of the final stage with magnetic refrigeration and realizes exhaust heat to room temperature by gas circulation cooling. Considering cooling the object to be cooled to the 20 to 40 K level, DyNi2 was selected as a magneto caloric material with high magnetic refrigeration characteristics (Magnetic entropy change $-\Delta S_m$ [J / (mol · K)] and adiabatic temperature change $\Delta T_{ad}$ [K]) in the temperature range around it [5]. Figure 7 shows the approximate magnetic entropy change $-\Delta S_m$ and adiabatic temperature change $\Delta T_{ad}$ in $DyNi_2$

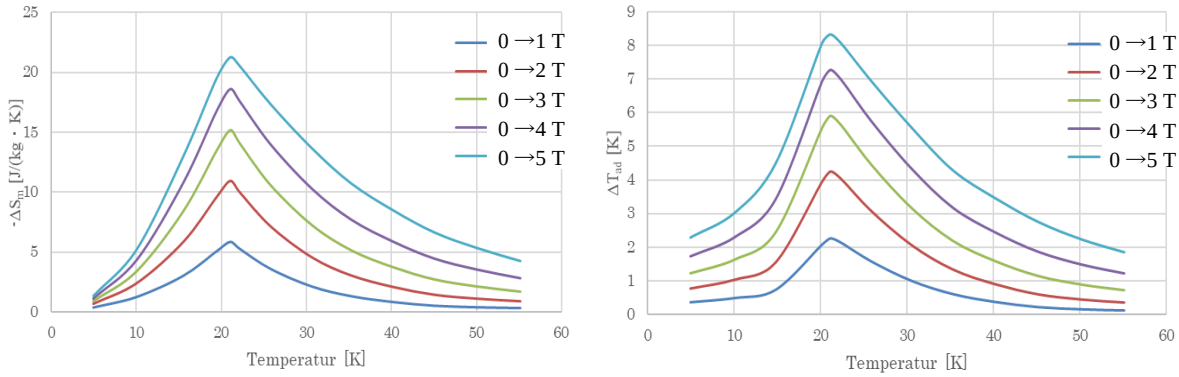


**Figure 7.** Approximate magnetic entropy change $-\Delta S_m$ and adiabatic temperature change $\Delta T_{ad}$ in $DyNi_2$

*4.2. One-dimensional numerical analysis model of gas circulation cooling system in combination with magnetic refrigerator*

Figure 8 shows an analysis model of a cooling system that combines a gas circulation cooling with cryogenic magnetic refrigerator. The analysis was performed by adding a cryogenic magnetic refrigerator mesh just before the heat input part of the one-dimensional numerical analysis model of the helium circulation cooling system. The analysis related to the magnetic refrigeration cycle was calculated by Equations (5) - (8) using $-\Delta S_m$ and $\Delta T_{ad}$. Where $Q_c$ is the amount of heat absorbed in one cycle [J], $Q_h$ is the amount of exhaust heat [J], $q_m$ is the refrigeration capacity of the magnetic refrigerator [W], $q_h$ is the amount of exhaust heat per second [w], $m_m$ is the mass of the magnetic refrigeration material [kg], f is the frequency of the magnetic refrigeration cycle [Hz]. Other calculation formulas are the same as those of the gas circulation refrigeration system.

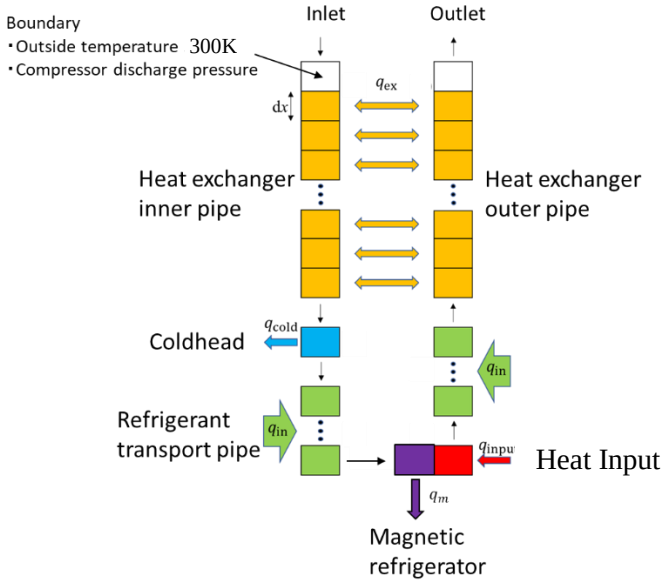


**Figure 8.** One-dimensional numerical analysis model of gas circulation cooling system in combination with magnetic refrigerator

$$Q_c = \frac{T+(T-\Delta T_{ad})}{2} * m_m * (-\Delta S_m) \quad (5)$$

$$Q_h = \frac{T+(T+\Delta T_{ad})}{2} * m_m * (-\Delta S_m) \quad (6)$$

$$q_m = Q_c * f \quad (7)$$

$$q_h = Q_h * f \quad (8)$$

Table 2 shows analysis parameters related to magnetic refrigeration. Other analysis parameters are the same as in Table 1.

**Table 2** The conditions of the numerical analysis for magnetic refrigeration

| | |
|---|---|
| Changes in magnetic field applied to magneto caloric materials | 1→3 T |
| Mass of magneto caloric materials | 0.23 kg |
| Magnetic refrigeration cycle frequency | 1 Hz |

*4.3. Numerical analysis results*

Figure 9 shows the analysis result. The dotted line in the figure shows the refrigeration performance of the cryogenic refrigerant circulation system when using a magnetic refrigerator, and the solid line shows the refrigeration performance without using a magnetic refrigerator.

It can be seen that the temperature of the cooled part with respect to the heat load is lowered by using the magnetic refrigerator. The refrigerating capacity when using a magnetic refrigerator in the temperature range of less than 45 K at 0.5 g/s is particularly high compared to when not using a magnetic refrigerator. The reason for this is that since the temperature was near the Curie temperature, the amount of magnetic entropy change and the amount of change in adiabatic temperature increased, and the performance of the magnetic refrigerator was fully demonstrated. At a flow rate of 1.5 g/s or higher, the temperature of the cooled part did not change much depending on whether a magnetic refrigerator was used or not. This is probably because the GM refrigerator could not lower the temperature of the circulating gas to a temperature where the performance of the magnetic refrigerator was improved due to the high flow rate.

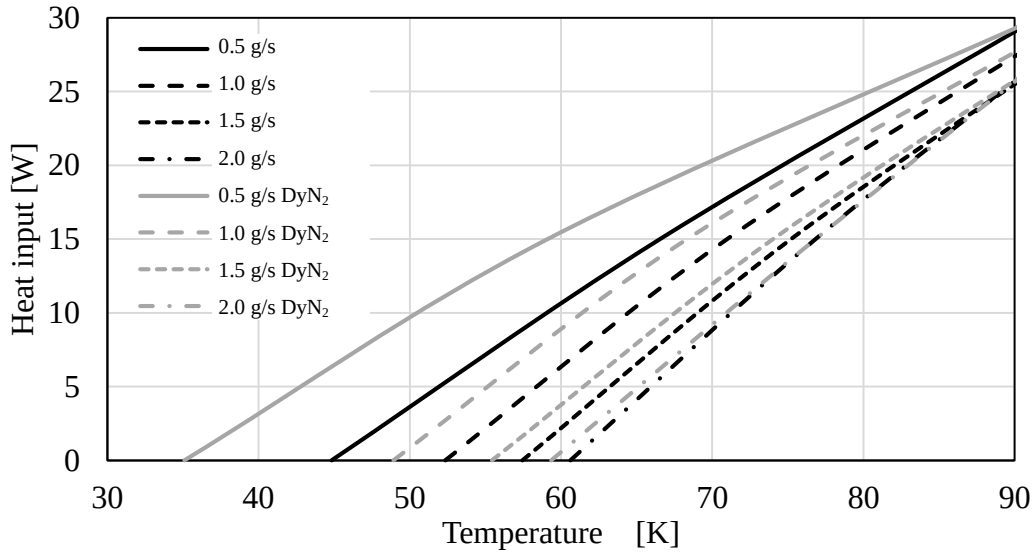


**Figure 9.** Cooled part temperature for heat load of gas circulation cooling combined with magnetic refrigerator

## 5. Summary

In order to clarify the temperature and flow characteristics of the cryogenic refrigerant circulation system and to improve the refrigeration performance, numerical analysis was performed.
The following conclusions were obtained from the results.

(1) In the refrigerant circulation cooling system, there is a refrigerant flow rate that maximizes the refrigeration performance with respect to the applied heat load, and the value increases as the heat load increases. However, if the flow rate is too high, the heat generation due to fluid friction occurs. Conversely, if the flow rate is too small, the heat conduction from the components that support the flow path in the device becomes dominant, so there is a range of values that can be taken as the optimal flow rate.
(2) It was suggested that a system that uses a magnetic refrigerator in combination with a refrigerant circulation cooling system may have higher refrigeration performance than a refrigerant circulation cooling system alone.

As the next step, we plan to compare the analysis results with basic experiments to confirm the accuracy of the analysis. In addition, the analysis will be performed by changing the circulating gas to hydrogen.

## References

[1] N. Hirano, S. Nagaya, M. Takahashi, T. Kuriyama, K. Ito, S. Nomura, Development of magnetic refrigerator for room temperature application, *Advances in Cryogenic Engineering*, 47, 1027-1034 (2002).
[2] T. Okamura, K. Yamada, N. Hirano, S. Nagaya, Performance of a room-temperature rotary magnetic refrigerator, *Proc.1st International Conference on Magnetic Refrigeration at Room Temperature*, IIF/IIR, 319-324 (2005).
[3] C. Zimm, A. Boeder, J. Chell, A. Sternberg, A. Fujita, S. Fujieda, K. Fukamichi, Design and performance of a permanent magnet rotary refrigerator, *Proc. 1st International Conference on Magnetic Refrigeration at Room Temperature*, IIF/IIR, 367- 373 (2005).
[4] Paulo V. Trevizoli, Theodor V. Christiaanse, Premakumara Govindappa, Iman Niknia, Reed Teyber, Jader R. Barbosa JR, Andrew Rome, Magnetic heat pumps: An overview of design principles and challenges, Science and Technology for the Built Environment 22, 507-519 (2016).
[5] P. J. von Ranke, V. K. Pecharsky and K. A. Gschneidner, Jr., Influence of the crystalline electricak field on the magnetocaloric effect of $DyAl_2$, $ErAl_2$ and $DyNi_2$, Physical Review B, Vol. 58, (1998).

## Acknowledgments

This work was supported by Chubu Electric Power Co., Inc. and JST ALCA Grant Number JPMJAL1408, Japan.